

REVIEW

Imaging of hepatocellular carcinoma: diagnosis, staging and treatment monitoring

Tiffany Hennedige^a, Sudhakar Kundapur Venkatesh^{a,b}

^a*Diagnostic Imaging, National University Hospital, National University Health System, Singapore;*

^b*Department of Radiology, Mayo Clinic, Rochester, MN, USA*

Corresponding address: Sudhakar K Venkatesh, MD, FRCR, Department of Radiology, Mayo Foundation and Clinic, 200, First Street SW, Rochester, MN 55905, USA.

Email: venkatesh.sudhakar@mayo.edu

Date accepted for publication 23 August 2012

Abstract

Hepatocellular carcinoma (HCC) is the most common primary liver cancer. Imaging is important for establishing a diagnosis of HCC. Several imaging modalities including ultrasonography (US), computed tomography (CT), magnetic resonance imaging (MRI), positron emission tomography (PET) and angiography are used in evaluating patients with chronic liver disease and suspected HCC. CT, MRI and contrast-enhanced US have replaced biopsy for diagnosis of HCC. Dynamic multiphase contrast-enhanced CT or MRI is the current standard for imaging diagnosis of HCC. Functional imaging techniques such as perfusion CT and diffusion-weighted MRI provide additional information about tumor angiogenesis that may be useful for treatment. Techniques evaluating tissue mechanical properties such as magnetic resonance elastography, and acoustic radiation force impulse imaging are being explored for characterizing liver lesions. The role of PET in the evaluation of HCC is evolving with promise seen especially with the use of a hepatocyte-specific PET tracer. Imaging is also critical for assessment of treatment response and detection of recurrence following locoregional treatment. Knowledge of the post-treatment appearance of HCC is essential for correct interpretation. This review article provides an overview of the role of imaging in the diagnosis, staging and post-treatment follow-up of HCC.

Keywords: *Hepatocellular carcinoma; CT; MRI; diagnosis; locoregional treatment.*

Introduction

Hepatocellular carcinoma (HCC) ranks sixth in cancer incidence and third in cancer mortality worldwide^[1]. It is the most common primary liver cancer with nearly three-quarters of cases in the world occurring in Asia secondary to the high prevalence of chronic viral hepatitis^[2]. Early diagnosis of HCC is important as several potentially curative treatment options are available that can then lead to an improved outcome. The early diagnosis of HCC hinges on its detection and diagnosis in accordance with the guidelines by the European Association for the Study of Liver Disease (EASL)^[3], American Association for the Study of Liver Diseases (AASLD)^[4], Asia-Pacific Association Study of the Liver (APASL)^[2], EASL-EORTC Clinical Practice Guidelines^[5] and the updated AASLD guidelines^[6]. Imaging tests are favored for surveillance and diagnosis

of HCC. Currently ultrasonography (US) is the recommended screening modality for periodic surveillance for HCC in at-risk patients. Dynamic and multiphase contrast-enhanced computed tomography (CT) and magnetic resonance imaging (MRI) are the standard diagnostic tests for HCC. Although the diagnosis of an HCC nodule >2 cm has acceptable accuracy, limitations in the detection and diagnosis of small HCCs still exist. Several advances and new imaging techniques are being explored for improved detection; characterization and staging of HCCs. Advances in CT include dual-energy CT (DECT) and perfusion CT (PCT). Faster MRI scanning, improved diffusion-weighted imaging (DWI) and hepatocyte-specific MR contrast agents are currently being explored. Emerging newer technologies such as MR elastography (MRE) and acoustic radiation force impulse imaging (ARFI) are promising for characterization of nodules in the liver. Positron emission

tomography (PET) with specific tracers may prove useful for staging of HCCs. Although liver transplantation and surgery are considered curative treatments for HCCs, more frequently and especially involving small HCCs, locoregional methods such as radiofrequency ablation (RFA) and ethanol ablation are now used. More advanced tumors may be treated with transarterial chemoembolization (TACE) and transarterial radioembolization (TARE). HCCs following locoregional treatment (LRT) can have variable appearances on CT and MRI and knowledge of post-treatment appearance is important for assessment of outcome and detection of residual or recurrent HCCs as there are no other reliable markers. Imaging therefore plays a crucial role in detection, diagnosis, staging and post-treatment follow-up of HCCs. This review presents an overview of the current status and advances in imaging diagnosis, staging and assessment of treatment response in HCC.

Epidemiology

HCC is associated with chronic liver disease and cirrhosis regardless of the etiology. Only about 10% of HCCs develop in non-cirrhotic livers^[7]. There is a growing incidence of HCC worldwide^[5]. A major risk factor is chronic infection with hepatitis B virus (HBV) or hepatitis C virus (HCV)^[8]. Chronic HBV infection is a leading cause of HCC in most Asian and African countries and HCV predominates in some southern European countries^[2]. Coinfection with HBV and HCV may have a synergistic effect on HCC development^[8]. Aside from chronic infection, there are important lifestyle factors that contribute to the development of HCC, namely, excess alcohol consumption, obesity, diabetes and intake of aflatoxin-contaminated foods^[9]. Alcohol intake increases the risk of HCC primarily through the development of cirrhosis. The principal route wherein obesity increases risk involves the association between obesity and non-alcoholic fatty liver disease (NAFLD)^[10]. Insulin resistance and the resulting inflammatory cascade along with the development of non-alcoholic steatohepatitis (NASH) appear to facilitate the development of HCC^[11]. Another significant lifestyle risk factor for hepatocarcinogenesis is the contamination of foodstuff with aflatoxin B1, which is produced by the fungus *Aspergillus flavus* and *A. parasiticus*^[12]. Cigarette smoking is considered a co-factor in the pathogenesis of HCC^[13]. The incidence of HCC also increases with HIV infection^[14]. Finally, genetic conditions such as hemochromatosis, alpha1-antitrypsin deficiency and glycogen storage disease type 1 are associated with a high risk of HCC, most often in the setting of cirrhosis^[15].

Surveillance for HCC

The most recent guidelines^[2–6] recommend US for surveillance of HCC at screening intervals of 6 months.

US has a sensitivity of 58–89% and specificity greater than 90%^[16,17]. US is performed in populations at risk such as cirrhotic patients, non-cirrhotic HBV carriers with active hepatitis or a family history of HCC, non-cirrhotic patients with chronic hepatitis C or advanced liver fibrosis. Tumor markers may be used in conjunction with US, however the sensitivity of serum alpha-fetoprotein (AFP) is low and results in additional detection of only 6–8% of cases with high false-positive results thereby increasing the cost of surveillance^[17–19]. The recent update in the AASLD guidelines therefore does not recommend serum AFP levels for surveillance and diagnosis^[6].

Small nodules less than 1 cm detected on US should be followed every 3–4 months in the first year and every 6 months thereafter^[5]. AASLD guidelines^[6] recommend a single diagnostic imaging test for HCC nodules >1 cm in cirrhotic patients, whereas the EASL-EORTC guidelines suggest a single diagnostic imaging test for nodules >2 cm and 2 diagnostic tests and/or biopsy for nodules between 1 and 2 cm for characterization. Some investigators have proposed the use of CT and MRI for HCC screening purposes as an alternative to US due to the difficulty with use in obese individuals and those with advanced cirrhosis^[20]. However, these modalities are not cost effective and there is the risk of cumulative radiation exposure from multiple CT scans^[21]. Hence, US is typically used as a surveillance tool for HCC detection in cirrhotic livers and CT or MRI for further evaluation if a nodule >1 cm is detected.

Diagnosis of HCC

Histological diagnosis of HCC is rarely required nowadays as non-invasive methods are preferred. HCC can be diagnosed in cirrhotic patients non-invasively on the basis of radiologic findings if imaging characteristics are present^[22]. CT, MRI and contrast-enhanced US (CEUS) are widely available and have largely replaced biopsy and conventional angiography for diagnosis of HCC. The diagnosis is based on the qualitative or visual appreciation of differences in attenuation on CT, echogenicity on CEUS and signal intensities on MRI of the HCC with respect to surrounding liver parenchyma. The imaging diagnosis of HCC can be done where state of the art CT and MRI machines are available with expertise in interpretation. Also, the diagnosis should be made on a dynamic multiphase contrast-enhanced study on a multi-detector row CT (MDCT) or MRI. The presence of arterial enhancement of a nodule 2 cm or more in size with subsequent washout on portal or delayed phases (Figs. 1, 2) are considered to be the definitive imaging features of HCC and recommended in the guidelines by various associations for liver studies^[2,4,23]. The washout refers to the hypodense or hypointense appearance of the HCC compared with that of the surrounding liver parenchyma. The cut-off size is 2 cm as pathology studies

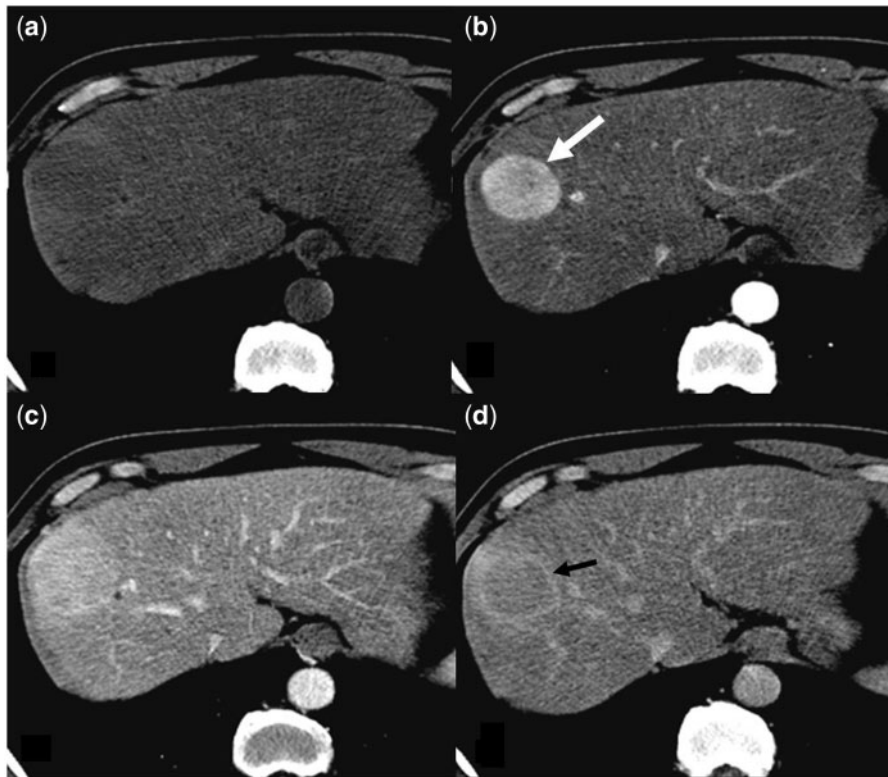


Figure 1 HCC in a 58-year-old man with chronic hepatitis B. Unenhanced (a), arterial phase (b), portal venous phase (c) and delayed phase (d) CT images showing a rounded HCC (white arrow) that enhances in arterial phase and washes out in portal venous and delayed phases. A thin enhancing pseudocapsule (black arrow head) is best demonstrated in the delayed phase.

have shown that the risk of microscopic vascular invasion and satellite nodules significantly increases when the tumor size exceeds 2 cm and has the characteristic arterial blood supply^[24]. Recent AASLD guidelines^[6] proposed that a single modality CT or MRI is sufficient when radiologic hallmark features are present in a nodule >1 cm. A second modality is needed when atypical features are present. Biopsy is performed if the nodule does not show typical features on 2 imaging techniques. However, EASL-EORTC guidelines^[5] consider a 1–2 cm nodule still problematic when atypical features are present and recommend histologic diagnosis. It is also recommended to have 2 techniques when the settings are suboptimal and expertise is not available. The role of CEUS in the diagnosis of HCC is still controversial and is not recommended due to low specificity^[25]. Frequently, 1–2 cm nodules do not show typical features of HCC^[26] and biopsy is required to establish the diagnosis and institute early treatment. The typical features may be present in only 26–62% of 1–2 cm HCCs using CEUS, CT or MRI alone^[23,27,28]. A non-negligible number of HCCs can be hypovascular and thereby lead to a false-negative diagnosis using the imaging criteria^[26]. Therefore, it may be useful to investigate atypical or hypovascular nodules >1 cm further with another

imaging technique or subject them to biopsy in order to rule out HCC. Nodules <1 cm have a low likelihood of being HCC and given the difficulty in obtaining a biopsy and limitations in the interpretation of these nodules by a pathologist, it is recommended that they are closely followed up using US until they grow to 1 cm or show atypical features making them eligible for further investigation^[4,23].

CT in HCC

Classic HCC shows arterial phase enhancement followed by a washout in the portal and/or delayed phase with a pseudocapsule around the nodule (Fig. 1). The other typical imaging features include internal mosaic pattern (Fig. 3), presence of fat (Fig. 4), vascular invasion (Fig. 5) and interval growth of 50% or more on serial images obtained less than 6 months apart^[29]. On unenhanced images, the appearance of HCC is variable and depends on the surrounding liver parenchyma and etiology of chronic liver disease. Most often, HCCs appear hypodense or isodense (Fig. 1) to the liver on unenhanced images but may appear hyperdense when they develop in a background of fatty liver. Portal vein tumor thrombosis (PVTT) is a well-known complication

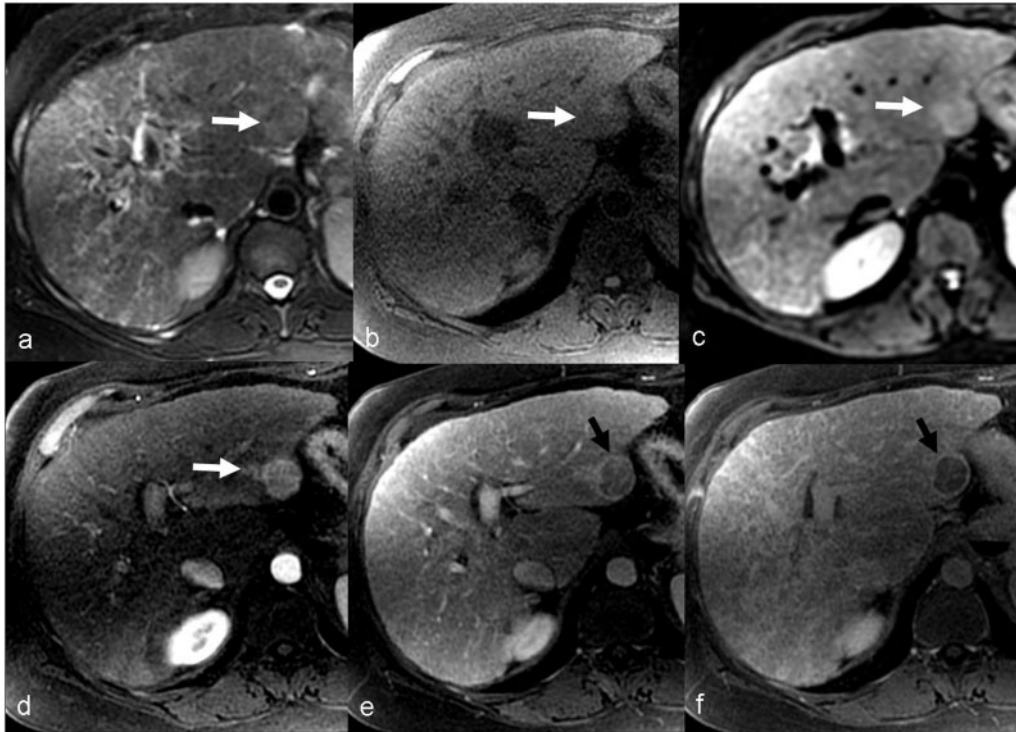


Figure 2 MRI of HCC in a 54-year-old woman with chronic hepatitis C. HCC (white arrow) appears mildly hyperintense to liver on the T2-weighted image (a), hypo- to isointense on the T1-weighted image, shows restricted diffusion on DWI (c), arterial phase enhancement (d) and washout in both portal venous (e) and delayed (f) phases. Note the enhancing capsule (black arrow) in both portal venous and delayed phases.

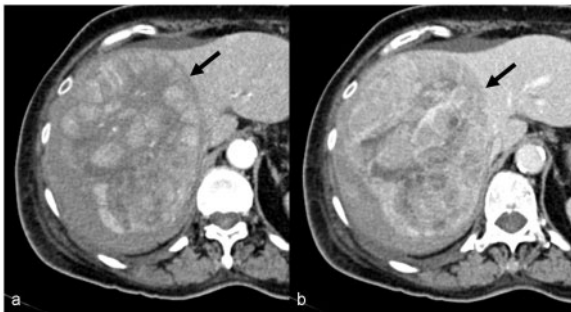


Figure 3 Large HCC (black arrow) in the right lobe of the liver showing heterogeneous enhancement in the arterial phase (a) and washout and mosaic appearance in the portal venous phase (b).

of HCC, the presence of which modifies typical imaging features (Figs. 5, 6). It is important to recognize these altered appearances for the purposes of accurate diagnosis and subsequent therapy. When HCC invades a portal vein or its branches, it continues to receive blood supply from the hepatic artery and may drain directly into the portal vein. This direct draining results in arteriportal

shunting and changes in portal vein hemodynamics. Large HCCs with PVTT less often demonstrate the typical arterial phase hypervascularity and subsequent washout diagnostic of HCC. Instead, the PVTT itself can show arterial phase enhancement and subsequent washout (Fig. 6) with distension of the vein^[30]. The portal vein demonstrates a cast of vessels, which represents neovascularity of the PVTT. The arteriportal shunting may also result in poor enhancement of the surrounding liver parenchyma.

Advances in CT

The introduction of MDCT has increased both the spatial and temporal resolution of CT making it possible to precisely evaluate the hemodynamics of liver tumors and liver parenchyma. Dynamic MDCT with high spatial and temporal resolution may be useful for reconstruction of three-dimensional images or even four-dimensional imaging, which is particularly advantageous for pretreatment evaluation of LRT. Some studies have shown that quadruple phase CT or double arterial phase (early arterial phase and late arterial phase) CT may improve the sensitivity of detection of HCC and result in fewer false-positive lesions than any one phase alone^[31,32]. The additional radiation dose needs to be considered when

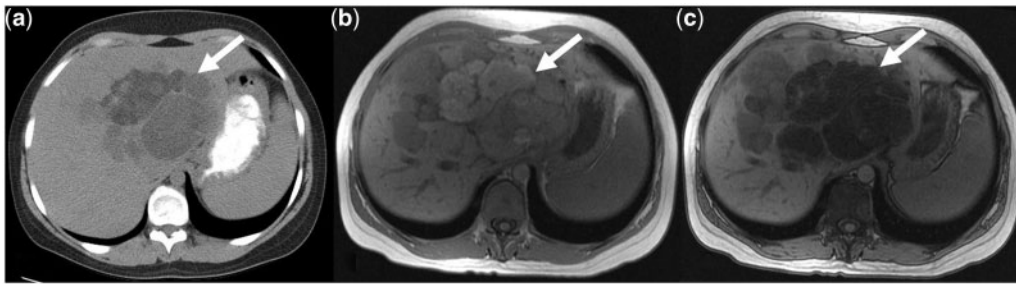


Figure 4 Fatty HCC. Unenhanced CT (a), in-phase (b) and opposed phase (c) MR images in the same patient showing heterogeneous HCC with fat component (arrow).

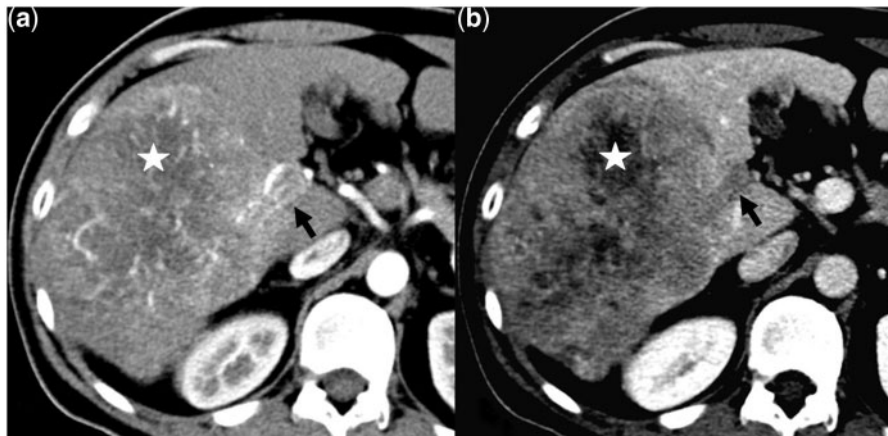


Figure 5 Large HCC (*) with portal vein invasion. Tumor thrombus within the portal vein (black arrow) showing enhancement in the arterial phase (a) and washout in the portal venous phase (b) similar to the main tumor.

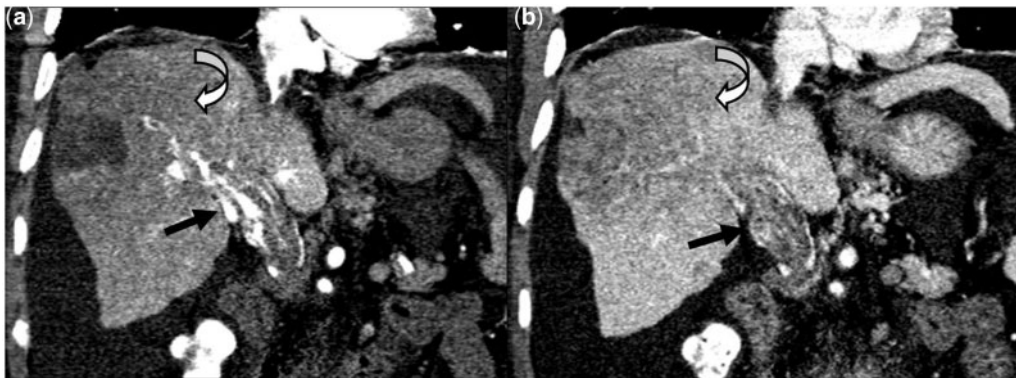


Figure 6 Large HCC with portal vein tumor thrombus. The portal vein is expanded and completely filled with tumor thrombus (black arrow). The tumor thrombus demonstrates neovascularity of cast of vessels in the arterial phase (a) and washout in the portal venous phase (b). The primary tumor (curved arrow) does not show arterial phase enhancement but appears hypodense in the both phases.

performing quadruple phase CT and studies have shown that late arterial phase CT is superior and adequate, with no significant benefit of an early arterial phase^[33,34].

Perfusion CT

Perfusion CT (PCT) enables detailed analysis of liver hemodynamics and quantitative information about tumor-related angiogenesis. PCT is performed by the acquisition of serial images after the administration of a bolus of iodinated contrast agent. Perfusion CT can measure tissue perfusion parameters quantitatively and can assess segmental hepatic function. PCT can also provide quantitative information about arterial perfusion in early HCCs and the perfusion parameters are significantly different in HCC tissue compared with surrounding liver parenchyma^[35,36].

Analysis of the microcirculation by perfusion CT may be useful in the evaluation of response to therapy, especially tumor response to anti-angiogenic drugs^[37,38]. Liver PCT has generally been performed for a single slice through the liver; however, high temporal resolution of volume helical shuttle (VHS) scanning enables whole liver perfusion imaging with multiple sections^[39]. VHS may be useful as a navigation tool for therapy such as transarterial chemoembolization. However, the limitations of PCT include increased radiation and lower resolution, which may be possible to overcome with low-dose CT protocols.

Dual-energy CT

Dual-energy CT enables differentiation of materials and tissues based on their CT density values, using 2 different energy spectra. This method includes a low tube voltage CT technique that increases the contrast enhancement of vascular structures while simultaneously reducing radiation dose. Monochromatic CT images at 80 kVp may show a higher contrast-to-noise ratio for hypervascular HCCs and potentially improve the assessment and detection of hypervascular liver tumors^[39]. CT image quality is strongly proportional to radiation dose. Several parameters such as milli-ampere (mA), exposure time, peak kilovoltage (kVp) and pitch need to be adjusted based on the relation between benefit and risk to the patient. Currently there are no large studies demonstrating benefit of dual-energy CT over conventional MDCT.

MRI of HCC

HCCs can have a variable appearance on MRI. Most HCCs are mildly hyperintense (Fig. 2) or isointense compared with surrounding liver on T2-weighted images^[40,41]. However, T2-weighted imaging alone does not have sufficient accuracy to characterize HCCs. HCCs are variable on T1-weighted images but mostly hypointense. HCCs smaller than 1.5 cm tend to be isointense^[40]. T1 hyperintensity has been attributed to the

degree of tumoral differentiation, the presence of copper, iron or glycogen deposition and the presence of intratumoral lipid^[40,42].

Lipid can be diffusely distributed or seen as focal accumulations. In-phase and opposed phase images can show microscopic fat components within HCCs (Fig. 4) with fat-containing areas showing signal drop out^[43]. The heterogeneity or mosaic appearance of the large HCCs may be better seen on MRI (Fig. 4) compared with MDCT due to better soft tissue contrast. The diagnosis of HCCs with MRI is based mainly on the enhancement pattern on dynamic post gadolinium-enhanced scans as the signal intensity of unenhanced images is not characteristic and overlaps with other focal lesions.

Hepatocyte-specific contrast imaging

Newer contrast agents that specifically target hepatic cells have been introduced to improve the diagnosis of HCC. Superparamagnetic iron oxide (SPIO) particles are taken up by Kupffer cells of the reticuloendothelial system and they enhance with T2 and T2* relaxation leading to marked reduction in signal intensity of the liver tissue particularly on T2-weighted images^[44]. Kupffer cells are rarely present in HCCs, therefore, the tumor shows little or no uptake of SPIO and appears hyperintense to normal liver (Fig. 7).

SPIO-enhanced MR images improve the non-invasive diagnosis of HCCs compared with dynamic CT and MRI used alone^[45]. Combining SPIO-enhanced MR with dynamic MRI has been shown to significantly improve detection of HCCs, particularly small HCCs in transplantation candidates^[46]. The use of SPIO is limited as it is not a US Food and Drug Administration-approved contrast agent, is not available worldwide and its use is complex, adding to the cost and duration of the MRI study.

Gadoxetate dimeglumine (Gd-EOB-DTPA, Primovist[®] in Europe and Eovist[®] in the United States, Bayer HealthCare; and gadobenate dimeglumine (Gd-BOPTA, Multihance[®], Bracco, Milan, Italy) are 2 hepatocyte-specific contrast agents available for clinical studies. Both contrast agents can be injected as an intravenous bolus that can provide information on vascularity and then information about hepatocyte function at 20 min (Gd-EOB-DTPA) or >60 min (Gd-BOPTA) after injection. With Gd-EOB-DTPA, approximately 50% of the drug is transported through normal hepatocytes and excreted into the bile compared with only 5% of Gd-BOPTA. Furthermore, only a small dose of Gd-EOB-DTPA (0.025 mmol/kg) is required compared with 0.1 mmol/kg for Gd-BOPTA. Gd-EOB-DTPA therefore has significant advantages in terms of safety, timing of examination and potentially better contrast. In the case of HCC, Gd-EOB-DTPA-enhanced MR images show early uptake in the arterial phase, washout patterns at the equilibrium phase and lower signal intensity in the hepatobiliary phase (Fig. 8)^[47]. Gd-EOB-DTPA-enhanced MR imaging is useful for differentiating small HCCs from focal

nodular hyperplasia, regenerative nodules and vascular pseudolesions^[48–51]. Gd-EOB-DTPA has been shown to be beneficial compared with MDCT and unenhanced MRI especially for detection of smaller lesions or of HCCs in underlying cirrhotic liver^[52]. However, 5–10%

of HCCs are iso- or hyperintense to liver in the hepatocyte phase^[53,54], therefore the images need to be interpreted with caution especially when dynamic images are not characteristic for HCCs. Hepatocyte-specific contrast agents in MRI are useful in the characterization of small hypovascular or atypical lesions, especially well-differentiated HCCs^[55].

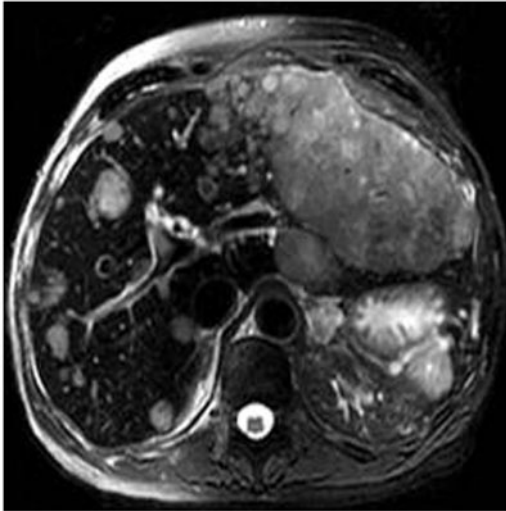


Figure 7 Multifocal HCCs well demonstrated using superparamagnetic iron oxide particle imaging. A T2-weighted image following SPIO administration shows a large mass in the left lobe and multiple smaller lesions in the right lobe.

Diffusion-weighted MR imaging

Diffusion-weighted imaging (DWI) offers insight into the molecular water composition and degree of tumor viability at the cellular level. Viable tumors are highly cellular and have intact cell membranes, thus restricting the motion of water molecules resulting in hyperintensity on DWI and reduction in the apparent diffusion coefficient (ADC)^[56]. DWI is particularly useful in initial screening of the liver as nearly 70–95% of HCCs can appear hyperintense^[57–59] (Figs. 2, 8) particularly using low b values. However, DWI may not be suitable for evaluating lesions near the dome of the liver secondary to magnetic susceptibility effects related to air in the lungs^[60]. DWI has a very high sensitivity for detection of nodules (Fig. 8), however ADC values used for characterization are not specific for differentiating HCC from dysplastic nodules as well as other malignant and benign lesions in the liver. Different ADC cutoffs have been reported with variable sensitivity of 74–100% and specificity of 77–100%^[61]. DWI, although not reliable in the differentiation of small nodules in cirrhotic liver may help

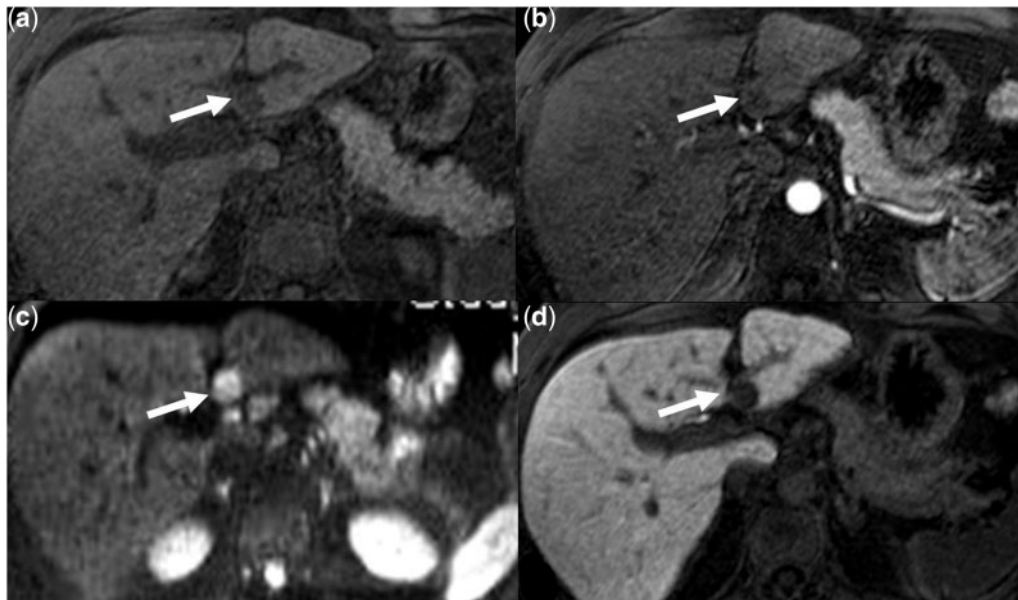


Figure 8 A 37-year-old man with chronic hepatitis B and raised AFP and histology proven HCC. Unenhanced (a) T1-weighted image showing a hypointense nodule (white arrow) in the left lobe and minimal enhancement in the arterial phase (b) and appears hypointense on the portal venous and delayed phases (not shown). Features are not typical for HCC. However, the nodule shows restricted diffusion on DWI with $b = 500$ and no uptake in the hepatocyte phase (d) after intravenous Gd-EOB-DTPA injection.

increase the diagnostic performance of readers^[62] and provide additional information to differentiate HCCs from dysplastic nodules^[63]. However, DWI is usually outperformed by contrast-enhanced MRI^[64] for the detection and characterization of HCC. Xu et al.^[65] found that the combined use of DWI with conventional dynamic contrast-enhanced MRI provided higher sensitivities than conventional dynamic contrast-enhanced MRI alone in the recognition of small HCC lesions (<1 cm) with a detection rate of up to 96% for the combined and 68% for the conventional technique. Recently researchers have introduced an intra-voxel incoherent motion (IVIM) model imaging, which can derive diffusion and perfusion parameters from DWI^[66] and may be useful in the characterization and differentiation of focal liver lesions. Recently, Piana et al.^[58] proposed new MR imaging criteria including DWI with contrast-enhanced MRI to improve the diagnosis of HCC in chronic liver diseases. However, there is no consensus among researchers and institutions on the technique of DWI and the strength of diffusion (*b* value) to use, which hinders comparison of experience across institutions.

MR elastography

MR elastography (MRE) is an emerging non-invasive method for measuring the viscoelastic properties of tissues. Several studies have shown that hepatic fibrosis increases the elasticity or stiffness of the liver, which can be detected and staged by this technique^[67,68]. MRE has shown potential in the differentiation of malignant solid tumors from benign tumors. Malignant liver tumors including HCC (Fig. 9) show significantly greater mean shear stiffness than benign tumors, normal and fibrotic liver^[69]. More studies are required to validate the possible application of MRE in the diagnosis and follow-up of HCC.

MR spectroscopy

The application of MR spectroscopy (MRS) to liver diseases is a recent development as a result of advances in imaging equipment that can now allow single voxel MRS in one breath hold. Although MRS is finding its application in the quantification of liver fat content, its use in characterization and diagnosis of liver tumors is still in its infancy and research in this direction is ongoing.

CEUS

CEUS utilizes microbubbles that are confined to the intravascular space as opposed to contrast agents in CT and MRI that are rapidly cleared from the blood pool into the extracellular space. The stabilized microbubbles containing either air or compressed gases are cleared in the lungs, which is useful in patients with renal failure or reduced renal function. With CEUS, the diagnosis of HCC is done using the same imaging criteria of arterial

phase hypervascularity and portal or delayed phase wash-out. However, this pattern is seen only for a short time and comprehensive scanning of the entire liver is not possible^[70]. Jang et al.^[71] have shown that CEUS is sensitive to the detection of arterial hypervascularity (Fig. 10) with up to 87% of all HCCs detected. The sensitivity of CEUS is less than 50% for small tumors^[72,73]. Further drawbacks include operator dependence, body habitus in obese patients and a limited field of view, which does not allow for imaging of the entire liver during a particular contrast phase^[74]. CEUS imaging is better suited to a focused examination of a previously detected liver nodule as opposed to surveillance of the entire liver. Therefore, although US is routinely used as a screening tool for detection of HCC in cirrhotic livers, CEUS is more applicable for the characterization of a known lesion. In addition, CEUS may provide false-positive results in patients with cholangiocarcinoma^[75] and is therefore not recommended as a diagnostic test in both AASLD and EASL-EORTC guidelines.

Ultrasound elastography and ARFI

Ultrasound elastography is a relatively new imaging technique that allows non-invasive estimation and imaging of tissue elasticity distribution within biological tissues using conventional real-time ultrasound with modified software^[76]. Malignant tumors are stiffer than benign tumors and up to 100 times stiffer than normal soft tissue^[77]. Gheorghe et al.^[78] found that ultrasound elastography is a promising method for the non-invasive diagnosis of early HCC.

ARFI is a new ultrasound imaging modality for evaluation of tissue stiffness by radiation force-based imaging that is provided with conventional B-mode US^[79]. A high ARFI value is associated with malignancy and low ARFI values with benign lesions. However, recent studies have shown conflicting results with regard to the usefulness of this technique for the characterization of HCC with high ARFI values occurring in benign as well as in malignant liver lesions^[80,81]. Kwon et al.^[79], however, have shown usefulness in this technique for the detection of recurrent HCCs after radiofrequency ablation. The clinical utility of ARFI remains to be determined.

PET

PET using [¹⁸F]fluorodeoxyglucose (FDG) can be useful in the detection of extrahepatic metastases that are not seen with CT or MRI, however, it has a low sensitivity for small and/or well-differentiated HCCs located within the liver secondary to the high background liver uptake of FDG^[82], with FDG-PET missing 30–50% of HCC lesions^[83]. PET also provides information regarding tissue perfusion, including that of the liver, but the spatial resolution is low^[84]. Moderate to well-differentiated HCCs may sometimes show avid uptake of FDG

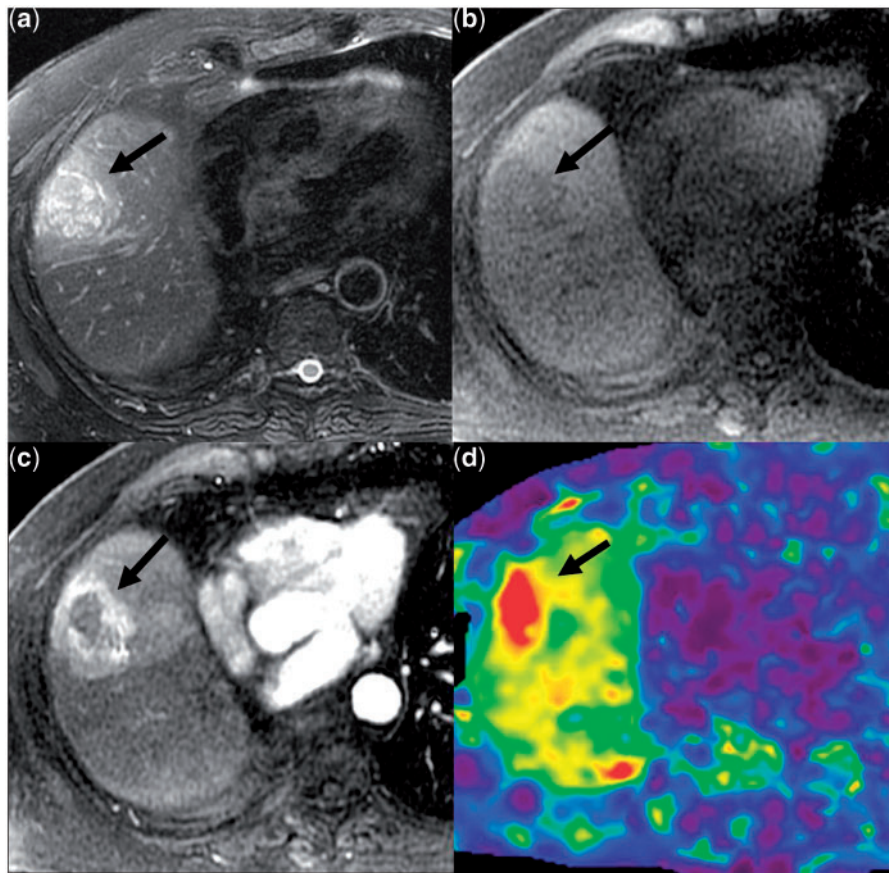


Figure 9 MR elastography of HCC in a background of cryptogenic liver cirrhosis. T2-weighted (a), unenhanced T1-weighted (b) and arterial phase (c) T1-weighted images showing typical HCC. Stiffness map from MR elastography (d) showing a high stiffness value of 10.6 kPa in the tumor. The stiffness of the liver parenchyma is 6.3 kPa, higher than the normal liver stiffness cut-off value of 2.93 kPa.

(Fig. 11). The use of dual-isotope PET (FDG and [^{11}C]acetate) may increase the sensitivity for HCC as well-differentiated tumors have a high avidity for acetate rather than glucose^[85]. However, a large prospective study comparing [^{11}C]acetate and FDG-PET/CT concluded that both tracers as well as the 2 tracers used in combination still had low sensitivity for the detection of small primary HCCs^[86]. A hepatocyte-specific PET tracer, 2- ^{18}F fluoro-2-deoxy-D-galactose (FDGal), which avidly accumulates in the liver compared with other tissues has shown promise in the detection of small intrahepatic HCC lesions that are poorly visualized by existing imaging methods^[83].

Other tests

Semi-invasive techniques such as hepatic angiography, angiography-assisted CT hepatic angiography (Fig. 12) or CT during arterial portography have fallen out of favor in most practice settings except in a few countries such as Japan^[87].

In addition to imaging techniques, early diagnosis of HCC can be made with biomarkers. The most commonly used serological marker is alpha-fetoprotein (AFP). However, sensitivity ranges from 25% for tumors <3 cm to 50% for lesions >3 cm in diameter^[88]. Other serum biomarkers and a new generation of IgM immunocomplexes have been tried with significant diagnostic limitations. However, simultaneous detection of these markers in various combinations could improve sensitivity^[88]. In addition, autoantibodies that have the ability to recognize the presence of abnormal tumor-associated antigens are promising biomarkers for the early detection of HCC^[89]. The biomarkers for HCC do not have sufficient accuracy for routine clinical use.

Staging of HCC

Staging and treatment of HCC depends on assessment of tumor extension or spread. Dynamic contrast-enhanced, multiphasic MRI and MDCT are the most effective techniques for detection and staging. Bone scintigraphy can be used for evaluating bone metastases. A complete

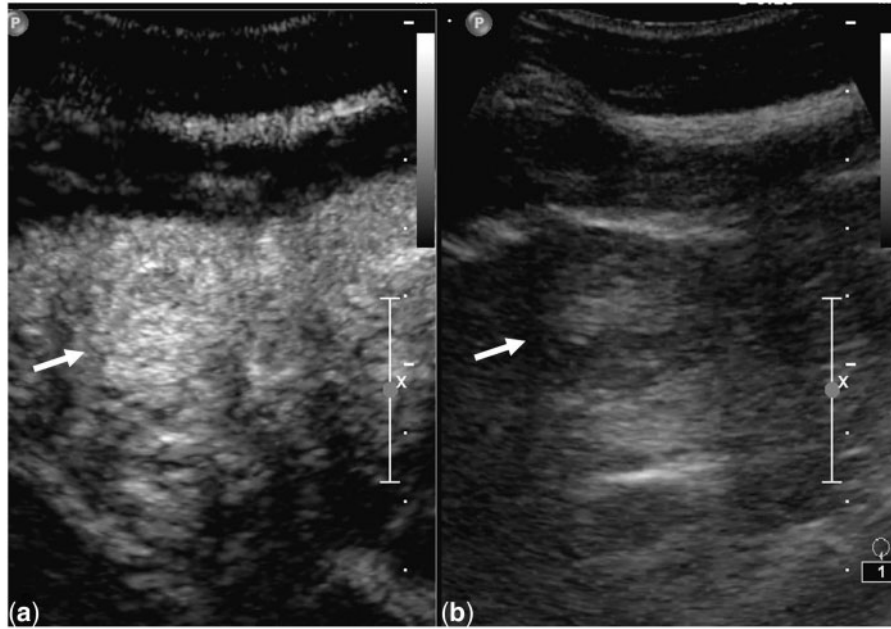


Figure 10 CEUS of HCC. Prompt intense enhancement of the segment 4 nodule (arrow) in the arterial phase (a) which is hypoechoic to surrounding liver on the grayscale image (b).

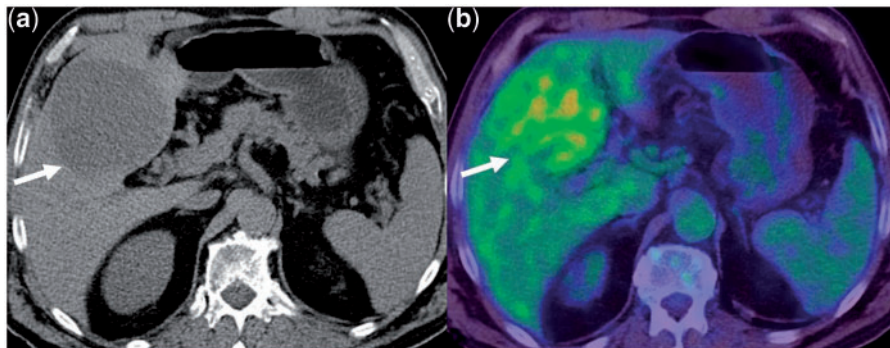


Figure 11 Unenhanced CT (a) and fused PET/CT image (b) of an FDG-avid moderately differentiated HCC (arrow).

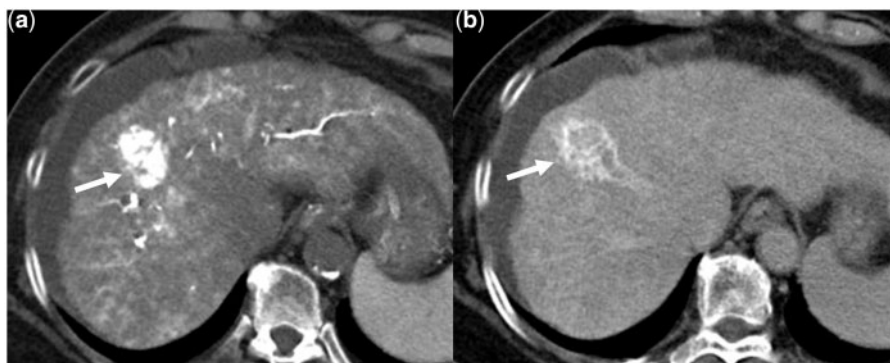


Figure 12 CT arteriography of HCC (arrow) in a 66-year-old patient with cryptogenic cirrhosis. Intense enhancement in the arterial phase (a) and washout in the central portion of the tumor in the delayed phase (b).

work-up of HCC patients includes dynamic contrast-enhanced CT or MRI, chest CT and bone scintigraphy. PET may be useful for staging the whole body and for resolving atypical features or doubtful metastases. Several staging systems are available and the Barcelona Clinic Liver Cancer (BCLC) classification is endorsed by the AASLD and EASL-EORTC guidelines. The BCLC classification^[90] includes tumor status, liver function and health performance status along with treatment-dependent variables and has been validated. The tumor status is defined by the size of the main nodule and multicentricity (single 2–5 cm, 3 nodules \leq 3 cm). CT and MRI play an important role in confirming the fact that tumors are solitary and remain single with no macrovascular involvement. Early stage tumors (BCLC stage A) have better survival with surgical resection, liver transplantation or local ablation in selected candidates. Intermediate HCCs (BCLC stage B) are usually treated with chemoembolization, and advanced HCCs receive chemotherapy.

Treatment options in HCC

Resection and liver transplantation have been the foundation of curative surgical treatment with the relatively recent advent of ablative techniques. Liver transplantation presents an opportunity to remove both the tumor and underlying chronic liver disease^[91], whereas resection may result in removal of vital functioning liver mass in an already compromised liver^[92]. Image-guided percutaneous ablation therapies have been widely performed on patients with small HCCs. They are potentially curative, minimally invasive and easily redone in cases of recurrence^[2].

HCCs exhibit strong neo-angiogenic activity during progression such that the tumor is mostly dependent on the hepatic artery for its blood supply^[2]. This specific arterial vascular profile provides the basis for therapeutic local chemotherapy and hepatic artery occlusion of HCCs by TACE^[93]. TACE can be used in patients with large/multifocal HCCs with no evidence of vascular invasion or extrahepatic spread and for down-staging tumors that exceed the criteria for transplantation^[94]. Recently, embolic drug-eluting beads have been developed that provide an alternative to conventional lipiodol-based regimens. The beads loaded with chemotherapeutic agent result in a combined ischemic and cytotoxic effect locally and low systemic toxic exposure^[95]. Transarterial radioembolization (TARE) is a form of brachytherapy in which intra-arterially injected yttrium 90 (⁹⁰Y) microspheres serve as sources of internal radiation^[96]. TARE is usually reserved for advanced HCCs or multifocal HCCs and unsuitable for other local ablation therapies. TARE treatment has been successful in reducing tumor burden in some advanced cases.

As mentioned previously, PVTT is a well-known complication of HCC, the presence of which alters the treatment strategy. The degree of shunting and associated changes in portal flow dynamics can have direct consequences on LRT. If an arteriportal shunt is present, the embolic material may get diverted to other branches of the portal vein and hence to non-tumor-bearing portions of the liver. Liver failure may be precipitated secondary to reduced arterial flow with transarterial therapy as the portal vein is already obstructed or there is reversed flow. TARE with its microembolic properties has been favored for the treatment of HCC with PVTT. TACE can also be performed safely for palliative tumor control in patients with advanced HCC with portal vein thrombosis^[97].

Assessment of treatment outcome after LRT

An understanding of the post-treatment imaging features with various imaging modalities is vital for assessment of treatment response and decisions on future therapy. Initially, the Response Evaluation Criteria in Solid Tumours (RECIST) guidelines were proposed for measuring the treatment response according to tumor shrinkage. However, the conventional RECIST takes into account only the overall diameter of a nodule, which is usually misleading when applied to LRT of HCC as treatment-induced changes in tissue viability often do not result in corresponding changes in lesion size^[98]. Hence, a modified RECIST (mRECIST) has been developed for evaluation of treatment response in HCC; only well-delineated arterially enhancing lesions can be selected as target lesions for mRECIST evaluation^[98].

Follow-up imaging with multiphasic CT or MRI should be performed 1–3 months after treatment to establish the need for further treatment^[74]. Contrast-enhanced CT is the most frequently used imaging modality secondary to its relative accessibility, robustness and ability to scan the chest and abdomen in one setting^[99]. Tumor ablation results in an area of necrosis, which appears as an area of hypodensity (Fig. 13) that may exhibit a thin, uniform peripheral rim of contrast enhancement in the arterial and/or portal venous phases, which may represent reactive hyperemia or granulation tissue^[2]. At MRI, necrosis after tumor ablation demonstrates low and high signal intensity on T2- and T1-weighted imaging (Fig. 14), respectively, due to coagulation necrosis^[99]. Hyperintensity on T1-weighted images may be due to hemorrhage or proteinaceous material within the ablated area^[102]. The higher sensitivity of MRI over CT is mostly due to the T2-weighted images; complete ablation would result in hypointensity with viable tumor appearing hyperintense^[100]. However, cystic necrosis of tumor may also demonstrate hyperintensity on T2-weighted imaging; therefore, in order to detect viable tumor, gadolinium-enhanced dynamic T1-weighted gradient recalled echo sequences are also used^[99]. In contrast, areas of nodular

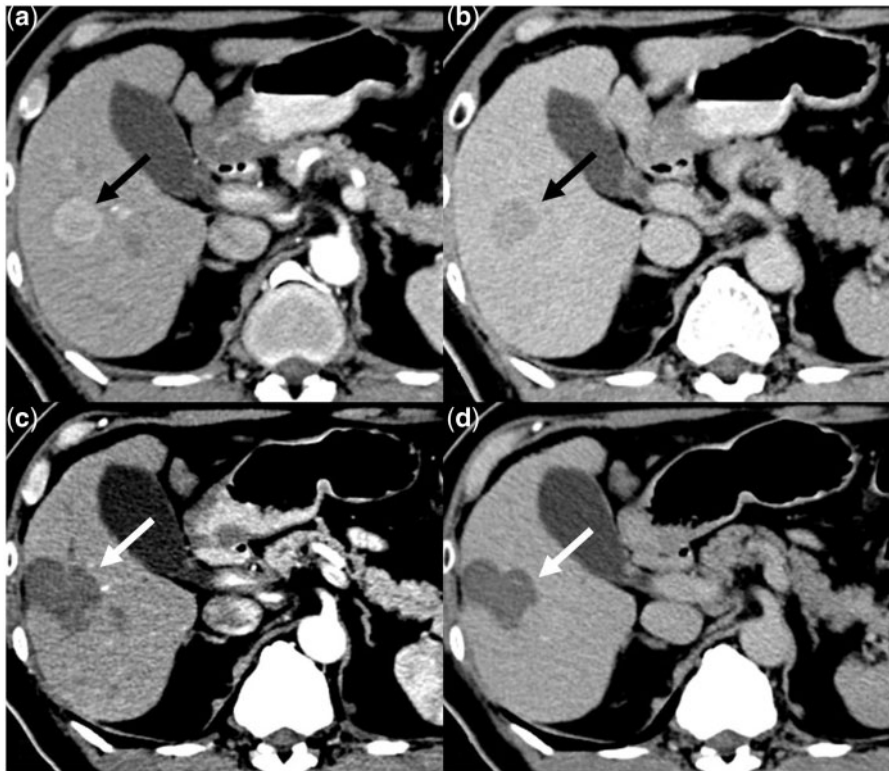


Figure 13 CT appearances before and after RFA of HCC. Top row: arterial (a) and portal venous phase (b) CT images showing an HCC (black arrow) before RFA. Bottom row: CT after 6 weeks of ablation; the HCC is replaced by a zone of hypodensity that is larger than the tumor and shows no enhancement (white arrow) in both the arterial (c) and portal venous phase (d).

or crescentic enhancing tissue in close proximity to the ablated lesion (Fig. 15) is suspicious of residual or recurrent HCC^[74]. Also, peripheral enhancement that becomes hypodense in the equilibrium phase is more suspicious of residual or recurrent tumor^[100]. Evaluation of the pretreatment scan could help to distinguish viable tumor as a side-by-side comparison could demonstrate whether the area of necrosis completely covers the tumor seen on pretreatment imaging^[99]. Non-tumorous wedge-like enhancement can also occur at the periphery of an ablated lesion secondary to iatrogenic arteriovenous shunting^[101].

TACE usually results in liquefaction necrosis and the tumor when adequately embolized shows no enhancement in follow-up imaging (Fig. 16). When lipiodol is used in conjunction with TACE, follow-up imaging with MRI may be the preferred modality as the extremely radiodense lipiodol may interfere with CT evaluation of marginal enhancement in residual or recurrent tumor^[74]. If subtraction techniques of unenhanced and contrast-enhanced images are not available, side-by-side assessment of unenhanced and contrast-enhanced CT scans is the standard technique to detect viable tumor^[99]. Focal washout of lipiodol during follow-up suggests the presence of viable tumor^[100]. Both CT and MRI have advantages and disadvantages for evaluation of LRT

efficacy, residual and recurrent disease. Several reports have demonstrated that dynamic MRI is more sensitive than CT for detection of lesions <2 cm^[103–105]. However, for the best possible comparability of images, serial post-treatment follow-up is ideally performed with the same modality used to assess the presence of the tumor before and after LRT^[74].

Post TARE results in liquefaction necrosis (Fig. 17) in the initial few weeks of follow-up without any decrease in the size of the lesions. Follow-up imaging may show reduction in the size of the lesions.

LRT results in cellular necrosis, which then causes increased membranous permeability allowing free diffusion of water molecules and resulting in reduced DWI and a marked increase in the ADC value^[56]. Kamel et al.^[60] found that DWI can quantify tumor necrosis after chemoembolization to a greater degree than gadolinium-enhanced MRI. Early after treatment with ⁹⁰Y, tumors demonstrate a decrease in enhancement and an increase in ADC, without a statistically significant change in tumor size^[106].

FDG-PET has also been shown to be of value in the detection of tumor recurrence after LRT^[3]. Potential drawbacks that may be encountered when using FDG-PET are false-negative results due to a partial volume effect when dealing with small lesions (<1 cm) or due

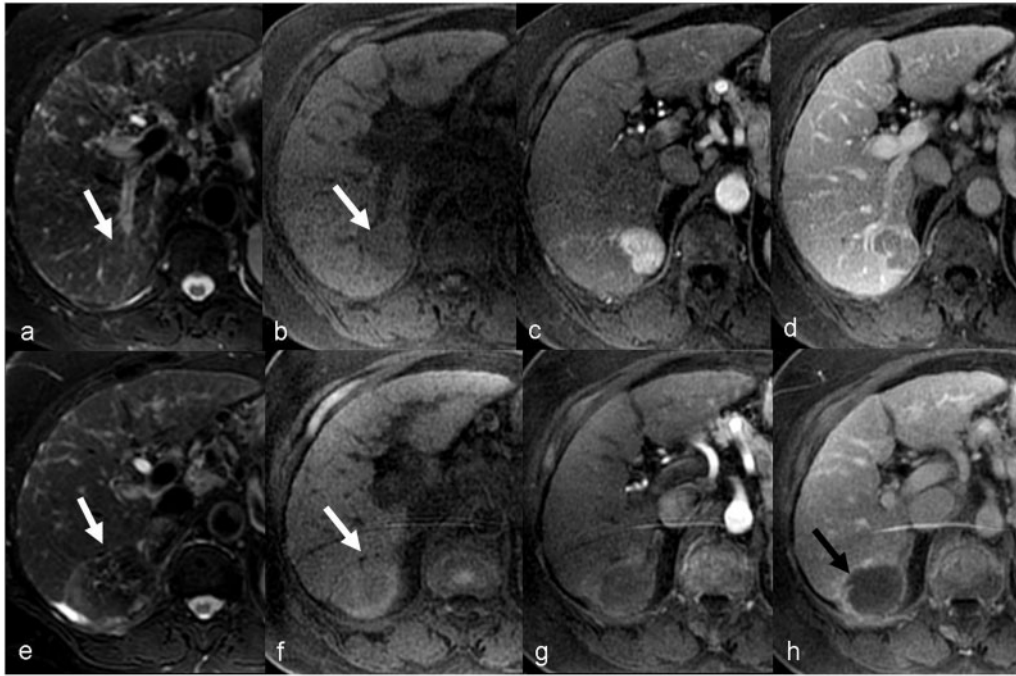


Figure 14 MR appearances of HCC before and after RF ablation. Before ablation (a–d), HCC is iso- to mildly hyperintense on the T2-weighted image (a), hypointense on the T1-weighted image (b), enhances in the arterial phase (c) and washes out in the portal venous phase (d). Post-ablation MRI (e–h) after 4 weeks showing a larger heterogeneous hypointensity on the T2-weighted image (e) and mixed hyperintensity on the T1-weighted image (f) representing the ablation zone (white arrows). There is no enhancement in the arterial phase (g) but a thin rim of post-ablation inflammatory enhancement (black arrow) seen in the portal venous phase (h).



Figure 15 Examples of post-RFA recurrence. Top row (a–c), a case of HCC (black arrow) in the background of non-alcoholic steatohepatitis and cirrhosis. Arterial phase CT before (a), 3 months after (b) and 1 year (c) after RFA. There is no recurrence at 3 months and the large ablation zone covers the tumor region. Nodular recurrence (white arrowheads) seen at 1 year at the margins of the ablation zone. Bottom row (d–f) is another example of nodular recurrence at the margin of the RFA zone illustrated on MRI. The recurrence is seen as hyperintense nodule on the T2-weighted image (d) and hypointense nodule on the T1-weighted image (e) in contrast to the ablated zone (curved arrow) and enhances in the arterial phase (f). (Image courtesy of Dr Grant Schmitt, MD, Mayo Clinic, Rochester, MN, USA.)

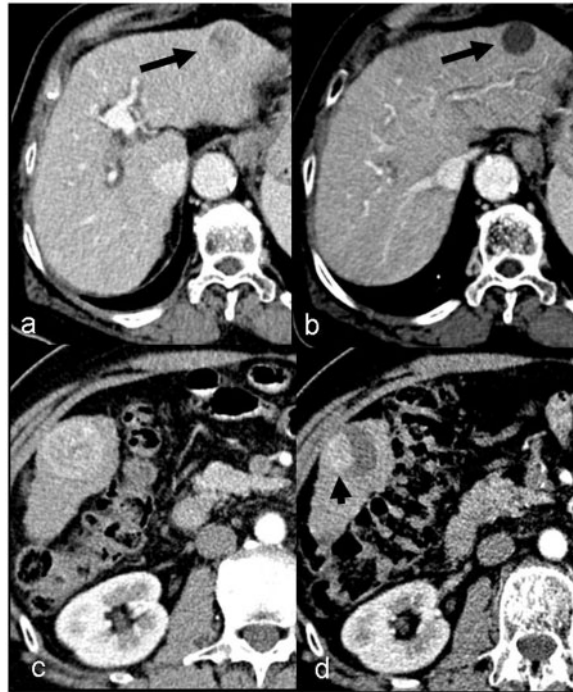


Figure 16 Examples of complete and partial response to TACE. Top row (a,b) showing a small HCC in the left lobe before (a) and 4 weeks after (b) TACE. There is mild reduction in the size of the tumor and no enhancement (black arrow). Bottom row (c,d) showing an HCC in the right lobe of the liver before (c) and 4 weeks after (d) TACE with residual tumor (black arrow head) seen in the post-TACE scan.



Figure 17 Examples of post-TARE response. Top row (a,b) showing arterial phase CT before (a) and 8 weeks after (b) TARE of a segment 6 HCC. There is complete necrosis of the tumor. (c,d) Arterial phase CT images in a patient with multifocal HCCs and partial response to TARE at 6 weeks. There is partial necrosis of the tumor (black arrowheads) and progression of tumor in segment 4 (white arrow).

to diabetes and false-positive results due to abscess formation^[3]. Another advantage of using FDG-PET after LRT is that, not only is it useful for ruling out recurrent HCC but it is also useful in ruling in extrahepatic metastases^[108]. In addition, Paudyal et al.^[109] found that FDG-PET detected recurrence earlier than CT with a higher overall detection rate (92% for FDG-PET compared with 75% for CT).

Summary

Potentially curative treatment is essentially limited to small HCCs. Therefore, ongoing research into the detection and characterization of small lesions is especially important. Dynamic imaging with CT or MRI is the mainstay of diagnosis of HCC. However, when imaging features are inconclusive, several other non-invasive imaging options are available. DWI and hepatocyte-specific MRI contrast agents are increasingly used in routine clinical practice and show great promise in improving imaging diagnosis and assessment of post-treatment outcome. PET/CT as well as MRE and US elastography are emerging techniques, and they may have a more pertinent role in the routine diagnosis of HCC in the near future as diagnostic accuracy of these techniques may improve.

References

- [1] Ferlay J, Shin HR, Bray F, Forman D, Mathers C, Parkin DM. Estimates of worldwide burden of cancer in 2008: GLOBOCAN 2008. *Int J Cancer* 2010; 127: 2893–2917. doi:10.1002/ijc.25516. PMID:21351269.
- [2] Omata M, Lesmana LA, Tateishi R, et al. Asian Pacific Association for the Study of the Liver consensus recommendations on hepatocellular carcinoma. *Hepatol Int* 2010; 4: 439–474. doi:10.1007/s12072-010-9165-7. PMID:20827404.
- [3] Bruix J, Sherman M, Llovet JM, et al. Clinical management of hepatocellular carcinoma. Conclusions of the Barcelona-2000 EASL conference. European Association for the Study of the Liver. *J Hepatol* 2001; 35: 421–430. doi:10.1016/S0168-8278(01)00130-1. PMID:11592607.
- [4] Bruix J, Sherman M. Practice Guidelines Committee, American Association for the Study of Liver Diseases. Management of hepatocellular carcinoma. *Hepatology* 2005; 42: 1208–1236. doi:10.1002/hep.20933. PMID:16250051.
- [5] European Association for the Study of the Liver, European Organization for Research and Treatment of Cancer. EASL-EORTC clinical practice guidelines: management of hepatocellular carcinoma. *J Hepatol* 2012; 56: 908–943.
- [6] Bruix J, Sherman M. American Association for the Study of Liver Diseases. Management of hepatocellular carcinoma: an update. *Hepatology* 2011; 53: 1020–1022. doi:10.1002/hep.24199. PMID:21374666.
- [7] Simonetti RG, Camma C, Fiorello F, Politi F, D'Amico G, Pagliaro L. Hepatocellular carcinoma. A worldwide problem and the major risk factors. *Dig Dis Sci* 1991; 36: 962–972. doi:10.1007/BF01297149. PMID:1649041.
- [8] Ferenci P, Fried M, Labrecque D, et al. World Gastroenterology Organisation global guideline. Hepatocellular carcinoma (HCC): a global perspective. *J Gastrointest Liver Dis* 2010; 19: 311–317. PMID:20922197.
- [9] Polesel J, Zucchetto A, Montella M, et al. The impact of obesity and diabetes mellitus on the risk of hepatocellular carcinoma. *Ann Oncol* 2009; 20: 353–357. doi:10.1093/annonc/mdn565. PMID:18723550.
- [10] Sanyal AJ, Yoon SK, Lencioni R. The etiology of hepatocellular carcinoma and consequences for treatment. *Oncologist* 2010; 15(Suppl 4): 14–22. doi:10.1634/theoncologist.2010-S4-14. PMID:21115577.
- [11] Montella M, Crispo A, Giudice A. HCC, diet and metabolic factors. *Hepat Mon* 2011; 11: 159–162. PMID:22087137.
- [12] El-Serag HB. Translational research: the study of community effectiveness in digestive and liver disorders. *Gastroenterology* 2007; 132: 8–10. doi:10.1053/j.gastro.2006.11.038. PMID:17241853.
- [13] Trichopoulos D, Bamia C, Lagious P, et al. Hepatocellular carcinoma risk factors and disease burden in a European cohort: a nested case-control study. *J Natl Cancer Inst* 2011; 103: 1686–1695. doi:10.1093/jnci/djr395. PMID:22021666.
- [14] Marcellin P, Pequignot F, Delarocque-Astagneau E, et al. Mortality related to chronic hepatitis B and chronic hepatitis C in France: evidence for the role of HIC coinfection and alcohol consumption. *J Hepatol* 2008; 48: 200–207. doi:10.1016/j.jhep.2007.09.010. PMID:18086507.
- [15] Dragani TA. Risk of HCC: genetic heterogeneity and complex genetics. *J Hepatol* 2010; 52: 252–257. doi:10.1016/j.jhep.2009.11.015. PMID:20022654.
- [16] Bolondi L. Screening for hepatocellular carcinoma in cirrhosis. *J Hepatol* 2003; 39: 1076–1084. doi:10.1016/S0168-8278(03)00349-0. PMID:14642630.
- [17] Singal A, Volk ML, Waljee A, et al. Meta-analysis: surveillance with ultrasound for early-stage hepatocellular carcinoma in patients with cirrhosis. *Ailment Pharmacol Ther* 2009; 30: 37–47. doi:10.1111/j.1365-2036.2009.04014.x.
- [18] Zhang B, Yang B. Combined alpha fetoprotein testing and ultrasonography as a screening test for primary liver cancer. *J Med Screen* 1999; 6: 108–110. PMID:10444731.
- [19] Lok AS, Sterling RK, Everhart JE, et al. Des-gamma-carboxy prothrombin and alpha-fetoprotein as biomarkers for the early detection of hepatocellular carcinoma. *Gastroenterology* 2010; 138: 493–502. doi:10.1053/j.gastro.2009.10.031. PMID:19852963.
- [20] Willatt JM, Hussain HK, Adusumilli S, Marrero JA. MR imaging of hepatocellular carcinoma in the cirrhotic liver: challenges and controversies. *Radiology* 2008; 247: 311–330. doi:10.1148/radiol.2472061331. PMID:18430871.
- [21] Andersson KL, Salomon JA, Goldie SJ, Chung RT. Cost effectiveness of alternative surveillance strategies for hepatocellular carcinoma in patients with cirrhosis. *Clin Gastroenterol Hepatol* 2008; 6: 1418–1424. doi:10.1016/j.cgh.2008.08.005. PMID:18848905.
- [22] Leoni S, Piscaglia F, Golferi R, et al. The impact of vascular and nonvascular findings on the noninvasive diagnosis of small hepatocellular carcinoma based on the EASL and AASLD criteria. *Am J Gastroenterol* 2010; 105: 599–609. doi:10.1038/ajg.2009.654. PMID:19935786.
- [23] Forner A, Vilana R, Ayuso C, et al. Diagnosis of hepatic nodules 20 mm or smaller in cirrhosis: prospective validation of the non-invasive diagnostic criteria for hepatocellular carcinoma. *Hepatology* 2008; 47: 97–104. doi:10.1002/hep.21966. PMID:18069697.
- [24] Kojiro M, Roskams T. Early hepatocellular carcinoma and dysplastic nodules. *Semin Liver Dis* 2005; 25: 133–142. doi:10.1055/s-2005-871193. PMID:15918142.
- [25] Rimola J, Forner A, Reig M, et al. Cholangiocarcinoma in cirrhosis: absence of contrast washout in delayed phases by magnetic resonance imaging avoids misdiagnosis of hepatocellular carcinoma. *Hepatology* 2009; 50: 791–198. doi:10.1002/hep.23071. PMID:19610049.
- [26] Bolondi L, Gaiani S, Celli N, et al. Characterization of small nodules in cirrhosis by assessment of vascularity: the problem

- of hypovascular hepatocellular carcinoma. *Hepatology* 2005; 42: 27–34. doi:10.1002/hep.20728. PMID:15954118.
- [27] Sangiovanni A, Manini MA, Iavarone M, et al. The diagnostic and economic impact of contrast imaging techniques in the diagnosis of small hepatocellular carcinoma in cirrhosis. *Gut* 2010; 59: 638–644. doi:10.1136/gut.2009.187286. PMID:19951909.
- [28] Luca A, Caruso S, Milazzo M, et al. Multidetector-row computed tomography (MDCT) for the diagnosis of hepatocellular carcinoma in cirrhotic candidates for liver transplantation: prevalence of radiological vascular patterns and histological correlation with liver explants. *Eur Radiol* 2010; 20: 898–907. doi:10.1007/s00330-009-1622-0. PMID:19802612.
- [29] Choi BI, Lee JM. Advancement in HCC imaging: diagnosis, staging and treatment efficacy assessments: imaging diagnosis and staging of hepatocellular carcinoma. *J Hepatobiliary Pancreat Sci* 2010; 17: 369–373. doi:10.1007/s00534-009-0227-y. PMID:19967573.
- [30] Shah ZK, McKernan MG, Hahn PF, Sahani DV. Enhancing and expansile portal vein thrombosis: value in the diagnosis of hepatocellular carcinoma in patients with multiple hepatic lesions. *AJR Am J Roentgenol* 2007; 188: 1320–1323. doi:10.2214/AJR.06.0134. PMID:17449777.
- [31] Murakami T, Kim T, Hori M, Federle MP. Double arterial phase multi-detector row helical CT for detection of hypervascular hepatocellular carcinoma. *Radiology* 2003; 229: 931–932. doi:10.1148/radiol.2293030590. PMID:14657326.
- [32] Schima W, Hammerstingl R, Catalano C, et al. Quadruple-phase MDCT of the liver in patients with suspected hepatocellular carcinoma: effect of contrast material flow rate. *AJR Am J Roentgenol* 2006; 186: 1571–1579. doi:10.2214/AJR.05.1226. PMID:16714645.
- [33] Kim SK, Lim JH, Lee WJ, et al. Detection of hepatocellular carcinoma: comparison of dynamic three-phase computed tomography images and four-phase computed tomography images using multidetector row helical computed tomography. *J Comput Assist Tomogr* 2002; 26: 691–698. doi:10.1097/00004728-200209000-00005. PMID:12439300.
- [34] Laghi A, Iannaccone R, Rossi P, et al. Hepatocellular carcinoma: detection with triple-phase multi-detector row helical CT in patients with chronic hepatitis. *Radiology* 2003; 226: 543–549. doi:10.1148/radiol.2262012043. PMID:12563152.
- [35] Ippolito D, Sironi S, Pozzi M, et al. Perfusion CT in cirrhotic patients with early stage hepatocellular carcinoma: assessment of tumor-related vascularization. *Eur J Radiol* 2010; 73: 148–152. doi:10.1016/j.ejrad.2008.10.014. PMID:19054640.
- [36] Sahani DV, Holalkere NS, Mueller PR, Zhu AX. Advanced hepatocellular carcinoma: CT perfusion of liver and tumor tissue-initial experience. *Radiology* 2007; 243: 736–743. doi:10.1148/radiol.2433052020. PMID:17517931.
- [37] Zhu AX, Holalkere NS, Muzihansky A, Horgan K, Sahani DV. Early antiangiogenic activity of bevacizumab evaluated by computed tomography perfusion scan in patients with advanced hepatocellular carcinoma. *Oncologist* 2008; 13: 120–125. doi:10.1634/theoncologist.2007-0174. PMID:18305056.
- [38] Ippolito D, Sironi S, Pozzi M, et al. Hepatocellular carcinoma in cirrhotic liver disease: functional computed tomography with perfusion imaging in the assessment of tumor vascularization. *Acad Radiol* 2008; 15: 919–927. doi:10.1016/j.acra.2008.02.005. PMID:18572129.
- [39] Okada M, Kim T, Murakami T. Hepatocellular nodules in liver cirrhosis: state of the art CT evaluation (perfusion CT/volume helical shuttle scan/dual-energy CT, etc.). *Abdom Imaging* 2011; 36: 273–281. doi:10.1007/s00261-011-9684-2. PMID:21267563.
- [40] Kelekis NL, Semelka RC, Worawattanakul S, et al. Hepatocellular carcinoma in North America: a multi-institutional study of appearance on T1-weighted, T2-weighted, and serial gadolinium-enhanced gradient-echo images. *AJR Am J Roentgenol* 1998; 170: 1005–1013. PMID:9530051.
- [41] Hussain HK, Syed I, Nghiem HV, et al. T2-weighted MR imaging in the assessment of cirrhotic liver. *Radiology* 2004; 230: 637–644. doi:10.1148/radiol.2303020921. PMID:14739306.
- [42] Ebara M, Fukuda H, Kojima Y, et al. Small hepatocellular carcinoma: relationship of signal intensity to histopathologic findings and metal content of the tumor and surrounding hepatic parenchyma. *Radiology* 1999; 210: 81–88. PMID:9885591.
- [43] Mitchell DG, Palazzo J, Hann HW, Rifkin MD, Burk DL Jr, Rubin R. Hepatocellular tumors with high signal on T1-weighted MR images: chemical shift MR imaging and histologic correlation. *J Comput Assist Tomogr* 1991; 15: 762–769. doi:10.1097/00004728-199109000-00007. PMID:1653279.
- [44] Imai Y, Murakami T, Yoshida S, et al. Superparamagnetic iron oxide-enhanced magnetic resonance images of hepatocellular carcinoma: correlation with histological grading. *Hepatology* 2000; 32: 205–212. doi:10.1053/jhep.2000.9113. PMID:10915725.
- [45] Yoo HJ, Lee JM, Lee JY, et al. Additional value of SPIO-enhanced MR imaging for the noninvasive imaging diagnosis of hepatocellular carcinoma in cirrhotic liver. *Invest Radiol* 2009; 44: 800–807. doi:10.1097/RLI.0b013e3181bc271d. PMID:19838119.
- [46] Lee DH, Kim SH, Lee JM, et al. Diagnostic performance of multidetector row computed tomography, superparamagnetic iron oxide-enhanced magnetic resonance imaging, and dual-contrast magnetic resonance imaging in predicting the appropriateness of a transplant recipient based on Milan criteria: correlation with histopathological findings. *Invest Radiol* 2009; 44: 311–321. doi:10.1097/RLI.0b013e31819c9f44. PMID:19462486.
- [47] Nasu K, Kuroki Y, Tsukamoto T, Nakajima H, Mori K, Minami M. Diffusion-weighted imaging of surgically resected hepatocellular carcinoma: imaging characteristics and relationship among signal intensity, apparent diffusion coefficient, and histopathologic grade. *AJR Am J Roentgenol* 2009; 193: 438–444. doi:10.2214/AJR.08.1424. PMID:19620441.
- [48] Kogita S, Imai Y, Okada M, et al. Gd-EOB-DTPA-enhanced magnetic resonance images of hepatocellular carcinoma: correlation with histological grading and portal blood flow. *Eur Radiol* 2010; 20: 2405–2413. doi:10.1007/s00330-010-1812-9. PMID:20490505.
- [49] Motosugi U, Ichikawa T, Sou H, et al. Distinguishing hypervascular pseudolesions of the liver from hypervascular hepatocellular carcinomas with gadoxetic acid-enhanced MR imaging. *Radiology* 2010; 256: 151–158. doi:10.1148/radiol.10091885. PMID:20574092.
- [50] Sano K, Ichikawa T, Motosugi U, Sou H, Muhi AM, Matsuda M. Imaging study of early hepatocellular carcinoma: usefulness of gadoxetic-acid-enhanced MR imaging. *Radiology* 2011; 261: 834–844. doi:10.1148/radiol.11101840. PMID:21998047.
- [51] Lee JM, Zech CJ, Bolondi L, et al. Consensus report of the 4th international forum for gadolinium-ethoxybenzyl-diethylenetriamine pentaacetic acid magnetic resonance imaging. *Korean J Radiol* 2011; 12: 403–415. doi:10.3348/kjr.2011.12.4.403. PMID:21852900.
- [52] Ichikawa T, Saito K, Yoshioka N, et al. Detection and characterization of focal liver lesions: a Japanese phase III, multicenter comparison between gadoxetic acid disodium-enhanced magnetic resonance imaging and contrast-enhanced computed tomography predominantly in patients with hepatocellular carcinoma and chronic liver disease. *Invest Radiol* 2010; 45: 133–141. doi:10.1097/RLI.0b013e3181caea5b. PMID:20098330.
- [53] Lee SA, Lee CH, Jung WY, et al. Paradoxical high signal intensity of hepatocellular carcinoma in the hepatobiliary phase of Gd-EOB-DTPA enhanced MRI: initial experience. *Magn Reson Imaging* 2011; 29: 83–90. doi:10.1016/j.mri.2010.07.019. PMID:20832227.
- [54] Tsuboyama T, Onishi H, Kim T, et al. Hepatocellular carcinoma: hepatocyte-selective enhancement at gadoxetic-acid-enhanced MR imaging-correlation with expression of sinusoidal and canalicular

- transporters and bile accumulation. *Radiology* 2010; 255: 824–833. doi:10.1148/radiol.10091557. PMID:20501720.
- [55] Kim MJ. Current limitations and potential breakthroughs for the early diagnosis of hepatocellular carcinoma. *Gut Liver* 2011; 5: 15–21. doi:10.5009/gnl.2011.5.1.15. PMID:21461067.
- [56] Kamel IR, Liapi E, Reyes DK, Zahurak M, Bluemke DA, Geschwind JF. Unresectable hepatocellular carcinoma: serial early vascular and cellular changes after transarterial chemoembolization as detected with MR imaging. *Radiology* 2009; 250: 466–473. doi:10.1148/radiol.2502072222. PMID:19188315.
- [57] Naganawa S, Kawai H, Fukatsu H, et al. Diffusion-weighted imaging of the liver: technical challenges and prospects for the future. *Magn Reson Med Sci* 2005; 4: 175–186. doi:10.2463/mrms.4.175. PMID:16543702.
- [58] Piana G, Trinquart L, Meskine N, Barrau V, Beers BV, Vilgrain V. New MR imaging criteria with a diffusion-weighted sequence for the diagnosis of hepatocellular carcinoma in chronic liver diseases. *J Hepatol* 2011; 55: 126–132. doi:10.1016/j.jhep.2010.10.023. PMID:21145857.
- [59] Vandecaveye V, De Keyser F, Verslype C, et al. Diffusion-weighted MRI provides additional value to conventional dynamic contrast-enhanced MRI for detection of hepatocellular carcinoma. *Eur Radiol* 2009; 19: 2456–2466. doi:10.1007/s00330-009-1431-5. PMID:19440718.
- [60] Kamel IR, Bluemke DA, Ramsey D, et al. Role of diffusion-weighted imaging in estimating tumour necrosis after chemoembolization of hepatocellular carcinoma. *AJR Am J Roentgenol* 2003; 181: 708–710. PMID:12933464.
- [61] Taouli B, Koh DM. Diffusion-weighted MR imaging of the liver. *Radiology* 2010; 254: 47–66. doi:10.1148/radiol.09090021. PMID:20032142.
- [62] Le Moigne F, Durieux M, Bancel B, et al. Impact of diffusion-weighted MR imaging on the characterization of small hepatocellular carcinoma in the cirrhotic liver. *Magn Reson Imaging* 2012; 30: 656–665. doi:10.1016/j.mri.2012.01.002. PMID:22459435.
- [63] Xu PJ, Yan FH, Wang JH, Shan Y, Ji Y, Chen CZ. Contribution of diffusion-weighted magnetic resonance imaging in the characterization of hepatocellular carcinomas and dysplastic nodules in cirrhotic liver. *J Comput Assist Tomogr* 2010; 34: 506–512. doi:10.1097/RCT.0b013e3181da3671. PMID:20657216.
- [64] Park MS, Kim S, Patel J, et al. Hepatocellular carcinoma: Detection with diffusion-weighted vs. contrast-enhanced MRI in pre-transplant patients. *Hepatology* 2012; 56: 140–148. doi:10.1002/hep.25681.
- [65] Xu PJ, Yan FH, Wang JH, et al. The value of breath-hold diffusion-weighted imaging in small hepatocellular carcinoma lesion (< or =3 cm) detection. *Zhonghua Yi Xue Za Zhi* 2009; 89: 592–596. PMID:19595157.
- [66] Taouli B, Ehman RL, Reeder SB. Advanced MRI methods for assessment of chronic liver disease. *AJR Am J Roentgenol* 2009; 193: 14–27. doi:10.2214/AJR.09.2601. PMID:19542391.
- [67] Yin M, Talwalkar JA, Glaser KJ, et al. A preliminary assessment of hepatic fibrosis with magnetic resonance elastography. *Clin Gastroenterol Hepatol* 2007; 5: 1207–1213. doi:10.1016/j.cgh.2007.06.012. PMID:17916548.
- [68] Huwart L, van Beers BE. MR elastography. *Gastroenterol Clin Biol* 2008; 32(Suppl. 1): 68–72. doi:10.1016/S0399-8320(08)73995-2. PMID:18973848.
- [69] Venkatesh SK, Yin M, Glockner JF, et al. MR elastography of liver tumours: preliminary results. *AJR Am J Roentgenol* 2008; 190: 1534–1540. doi:10.2214/AJR.07.3123. PMID:18492904.
- [70] Lencioni R, Piscaglia F, Bolondi L. Contrast-enhanced ultrasound in the diagnosis of hepatocellular carcinoma. *J Hepatol* 2008; 48: 848–857. doi:10.1016/j.jhep.2008.02.005. PMID:18328590.
- [71] Jang HJ, Kim TK, Burns PN, Wilson SR. Enhancement patterns of hepatocellular carcinoma at contrast-enhanced US: comparison with histologic differentiation. *Radiology* 2007; 244: 898–906. doi:10.1148/radiol.2443061520. PMID:17709836.
- [72] Lencioni R, Pinto F, Armillotta N, Bartolozzi C. Assessment of tumor vascularity in hepatocellular carcinoma: comparison of power Doppler US and color Doppler US. *Radiology* 1996; 201: 353–358. PMID:8888222.
- [73] Lencioni R, Mascalchi M, Caramella D, Bartolozzi C. Small hepatocellular carcinoma: differentiation from adenomatous hyperplasia with color Doppler US and dynamic Gd-DTPA-enhanced MR imaging. *Abdom Imaging* 1996; 21: 41–48. doi:10.1007/s002619900007. PMID:8672971.
- [74] Lee JM, Trevisani F, Vilgrain V, Wald C. Imaging diagnosis and staging of hepatocellular carcinoma. *Liver Transpl* 2011; 17 (Suppl 2): S34–43.
- [75] Rimola J, Forner A, Reig M, et al. Cholangiocarcinoma in cirrhosis: absence of contrast washout in delayed phases by magnetic resonance imaging avoids misdiagnosis of hepatocellular carcinoma. *Hepatology* 2009; 50: 791–798. doi:10.1002/hep.23071. PMID:19610049.
- [76] Gheorghe L, Iacob S, Georghe C. Real time sonoelastography- a new application in the field of liver disease. *J Gastrointest Liver Dis* 2008; 17: 469–474. PMID:19104713.
- [77] Rustemovic N, Hrstic I, Opacic M, et al. EUS elastography in the diagnosis of focal liver lesions. *Gastrointest Endosc* 2007; 66: 823–824. PMID:17681503.
- [78] Gheorghe L, Iacob S, Iacob R, et al. Real time elastography- a non-invasive diagnostic method of small hepatocellular carcinoma in cirrhosis. *J Gastrointest Liver Dis* 2009; 18: 439–446. PMID:20076816.
- [79] Kwon HJ, Kang MJ, Cho JH, et al. Acoustic radiation force impulse elastography for hepatocellular carcinoma-associated radiofrequency ablation. *World J Gastroenterol* 2011; 17: 1874–1878. doi:10.3748/wjg.v17.i14.1874. PMID:21528062.
- [80] Heide R, Strobel D, Bernatik T, Goertz RS. Characterization of focal liver lesions (FLL) with acoustic radiation force impulse (ARFI) elastometry. *Ultraschall Med* 2010; 31: 405–409. doi:10.1055/s-0029-1245565. PMID:20652853.
- [81] Gallotti A, D'Onofrio M, Romanini L, Cantosani V, Pozzi Mucelli R. Acoustic radiation force impulse (ARFI) ultrasound imaging of solid focal liver lesions. *Eur J Radiol* 2012; 81: 451–455. doi:10.1016/j.ejrad.2010.12.071. PMID:21330078.
- [82] Ho CL, Chen S, Yeung DW, Cheng TK. Dual-tracer PET/CT imaging in evaluation of metastatic hepatocellular carcinoma. *J Nucl Med* 2007; 48: 902–909. doi:10.2967/jnumed.106.036673. PMID:17504862.
- [83] Sorensen M, Frisch K, Bender D, Keiding S. The potential use of 2-[¹⁸F]fluoro-2-deoxy-D-galactosis as a PET/CT tracer for detection of hepatocellular carcinoma. *Eur J Nucl Med Mol Imaging* 2011; 38: 1723–1731. doi:10.1007/s00259-011-1831-z. PMID:21553087.
- [84] Nagamachi S, Czernin J, Kim AS, et al. Reproducibility of measurements of regional resting and hyperemic myocardial blood flow assessed with PET. *J Nucl Med* 1996; 37: 1626–1631. PMID:8862296.
- [85] Delbeke D, Martin WH. Update of PET and PET/CT for hepatobiliary and pancreatic malignancies. *HPB (Oxford)* 2005; 7: 166–179. doi:10.1080/13651820510028909.
- [86] Park JW, Kim JH, Kim SK, et al. A prospective evaluation of 18-F-FDG and 11C-acetate PET/CT for detection of primary and metastatic hepatocellular carcinoma. *J Nucl Med* 2008; 49: 1912–1921. doi:10.2967/jnumed.108.055087. PMID:18997056.
- [87] El-Serag HB, Marrero JA, Rudolph L, Reddy KR. Diagnosis and treatment of hepatocellular carcinoma. *Gastroenterology* 2008; 134: 1752–1763. doi:10.1053/j.gastro.2008.02.090. PMID:18471552.
- [88] Stefaniuk P, Cianciara J, Wiercinska-Drapalo A. Present and future possibilities for early diagnosis of hepatocellular carcinoma. *World J Gastroenterol* 2010; 16: 418–424. doi:10.3748/wjg.v16.i4.418. PMID:20101765.

- [89] Heo CK, Woo MK, Yu DY, et al. Identification of autoantibody against fatty acid synthase in hepatocellular carcinoma mouse model and its application to diagnosis of HCC. *Int J Oncol* 2010; 36: 1453–1459. PMID:20428769.
- [90] Llovet JM, Brú C, Bruix J. Prognosis of hepatocellular carcinoma: the BCLC staging classification. *Semin Liver Dis* 1999; 19: 329–338. doi:10.1055/s-2007-1007122. PMID:10518312.
- [91] Figueras J, Ibanez L, Ramos E, et al. Selection criteria for liver transplantation in early-stage hepatocellular carcinoma with cirrhosis: results of a multicenter study. *Liver Transpl* 2001; 7: 877–883. doi:10.1053/jlts.2001.27856. PMID:11679986.
- [92] Deshpande R, O'Reilly D, Sherlock D. Improving outcomes with surgical resection and other ablative therapies in HCC. *Int J Hepatol* 2011; doi:10.4061/2011/686074.
- [93] Bruix J, Sala M, Llovet JM. Chemoembolization for hepatocellular carcinoma. *Gastroenterology* 2004; 127: S179–188. doi:10.1053/j.gastro.2004.09.032. PMID:15508083.
- [94] Hanje AJ, Yao FY. Current approach to down-staging of hepatocellular carcinoma prior to liver transplantation. *Curr Opin Organ Transplant* 2008; 13: 234–240. doi:10.1097/MOT.0b013e3282fc2633. PMID:18685309.
- [95] Lencioni R, de Baere T, Burrel M, et al. Transcatheter treatment of hepatocellular carcinoma with doxorubicin-loaded DC bead (DEBDOX): technical recommendations. *Cardiovasc Intervent Radiol* 2012; 35: 980–985. doi:10.1007/s00270-011-0287-7. PMID:22009576.
- [96] van Malenstein H, Maleux G, Vandecaveye V, et al. A randomized phase II study of drug-eluting beads versus transarterial chemoembolization for unresectable hepatocellular carcinoma. *Onkologie* 2011; 34: 368–376. doi:10.1159/000329602. PMID:21734423.
- [97] Vogl TJ, Nour-Eldin NE, Emad-Eldin S, et al. Portal vein thrombosis and arterioportal shunts: effects on tumour response after chemoembolization of hepatocellular carcinoma. *World J Gastroenterol* 2011; 17: 1267–1275. doi:10.3748/wjg.v17.i10.1267. PMID:21455325.
- [98] Lencioni R, Llovet JM. Modified RECIST (mRECIST) assessment for hepatocellular carcinoma. *Semin Liver Dis* 2010; 30: 52–60. doi:10.1055/s-0030-1247132. PMID:20175033.
- [99] Schima W, Ba-Ssalamah A, Kurtaran A, Schindl M, Gruenberger T. Post-treatment imaging of liver tumours. *Cancer Imaging* 2007; 7(A): S28–36.
- [100] Guan YS, Sun L, Zhou XP, Li X, Zheng XH. Hepatocellular carcinoma treatment with interventional procedures: CT and MRI follow-up. *World J Gastroenterol* 2004; 10: 3543–3548. PMID:15534903.
- [101] Choi D, Lim HK, Kim SH, et al. Assessment of therapeutic response in hepatocellular carcinoma treated with percutaneous radio frequency ablation: comparison of multiphase helical computed tomography and power Doppler ultrasonography with a microbubble contrast agent. *J Ultrasound Med* 2002; 21: 391–401. PMID:11934096.
- [102] Shibata T, Iimuro Y, Yamamoto Y, et al. Small hepatocellular carcinoma: comparison of radio-frequency ablation and percutaneous microwave coagulation therapy. *Radiology* 2002; 223: 255–262.
- [103] Choi SH, Lee JM, Yu NC, et al. Hepatocellular carcinoma in liver transplantation candidates: detection with gadobenate dimeglumine-enhanced MRI. *AJR Am J Roentgenol* 2008; 191: 529–536. doi:10.2214/AJR.07.2565. PMID:18647927.
- [104] Kim YK, Kim CS, Chung GH, et al. Comparison of gadobenate dimeglumine-enhanced dynamic MRI and 16-MDCT for the detection of hepatocellular carcinoma. *AJR Am J Roentgenol* 2006; 186: 149–157. doi:10.2214/AJR.04.1206. PMID:16357395.
- [105] Taouli B, Krinsky GA. Diagnostic imaging of hepatocellular carcinoma in patients with cirrhosis before liver transplantation. *Liver Transpl* 2006; 12(Suppl 2): S1–7. doi:10.1002/lt.20935. PMID:17051556.
- [106] Kamel IR, Reyes DK, Liapi E, Bluemke DA, Geschwind JF. Functional MR imaging assessment of tumour response after 90Y microsphere treatment in patients with unresectable hepatocellular carcinoma. *J Vasc Interv Radiol* 2007; 18: 49–56. doi:10.1016/j.jvir.2006.10.005. PMID:17296704.
- [107] Dierckx R, Maes A, Peeters M, Van De Wiele C. FDG PET for monitoring response to local and loco regional therapy in HCC and liver metastases. *Q J Nucl Med Mol Imaging* 2009; 53: 336–342. PMID:19521313.
- [108] Lin CY, Chen JH, Liang JA, Lin CC, Jeng LB, Kao CH. 18F-FDG PET or PET/CT for detecting extrahepatic metastases or recurrent hepatocellular carcinoma: a systematic review and meta-analysis. *Eur J Radiol* 2012; 81: 2417–2422. doi:10.1016/j.ejrad.2011.08.004. PMID:21899970.
- [109] Paudyal B, Oriuchi N, Paudyal P, et al. Early diagnosis of recurrent hepatocellular carcinoma with 18F-FDG PET after radio-frequency ablation therapy. *Oncol Rep* 2007; 18: 1469–1473. PMID:17982632.